Atlas of Early Neoplasias of the Gastrointestinal Tract

Endoscopic Diagnosis and Therapeutic Decisions

Frieder Berr
Tsuneo Oyama
Thierry Ponchon
Naohisa Yahagi
Editors

Second Edition

Springer

Atlas of Early Neoplasias of the Gastrointestinal Tract

Frieder Berr • Tsuneo Oyama
Thierry Ponchon • Naohisa Yahagi
Editors

Atlas of Early Neoplasias of the Gastrointestinal Tract

Endoscopic Diagnosis and Therapeutic Decisions

Second Edition

Springer

Editors
Frieder Berr
Department of Internal Medicine I
Paracelsus Medical University
Salzburg
Austria

Thierry Ponchon
Department of Digestive Diseases
Hôpital Eduard Herriot
Lyon
France

Tsuneo Oyama
Department of Endoscopy
Saku Central Hospital Advanced Care Center
Saku
Nagano
Japan

Naohisa Yahagi
Division of Research and Development
for Minimally Invasive Treatment
Cancer Center
Keio University School of Medicine
Shinjuku-ku
Tokyo
Japan

ISBN 978-3-030-01113-0 ISBN 978-3-030-01114-7 (eBook)
https://doi.org/10.1007/978-3-030-01114-7

Library of Congress Control Number: 2019930836

This Springer imprint is published by the registered company Springer Nature Switzerland AG
The registered company address is: Gewerbestrasse 11, 6330 Cham, Switzerland

This book is dedicated to all colleagues who strive for proficiency in image-enhanced endoscopic analysis of early gastrointestinal cancers. Accurate endoscopic staging of superficial neoplasias results in correct indications for appropriate resection technique and serves the best interest of the patients.

Salzburg, August 15, 2018 *The Editors*

Preface

"**State-of-the-art endoscopic skills best serve the patient**"

Since the first edition of this endoscopy atlas and compendium of indications, endoscopic en bloc resection based on ESD techniques has proven equally curative for the resection of early GI cancers as major resective surgery. And the techniques are now refined for ESD of early cancer as well as for endoscopic tunneling resection of symptomatic or pre-/malignant early intramural tumors. Consequently, some Western guidelines have adopted the principle of endoscopic en bloc resection of malignant appearing GI neoplasias, whereas others still adhere to piecemeal snaring techniques for early cancer in Barrett's esophagus or colorectum – assigning diagnostic competence exclusively afterward to the histopathologist.

In the last decade, a network of pioneering referral centers throughout Western countries has reported on implementation of ESD technique. And the endoscopic electrosurgical performance – as taken by high rates of en bloc resection and low rates of emergency surgery and mortality – are nearly approaching East Asian standards. However, the rates of curative resection by ESD still lag behind East Asian standards due mainly to poor prediction of submucosal invasion and less to inadequate delineation of lateral margins or multiple foci of early cancer.

The updated and slightly extended second edition of this atlas on early GI neoplasias *aims* to increase *detection* of pre-/malignant neoplasias in the earliest stage, predict the *tumor category* with high accuracy, and *make the indication* for the least invasive curative resection technique based on this diagnosis. An effort is needed to accomplish professionalism and best serve the patients. The learning curve to professional image-enhanced endoscopy and accurate endoscopic diagnosis of early GI

cancers may take up to 2 years, until the technique becomes a rapid and accurate routine procedure. We publish this atlas and compendium for those who strive to accomplish state-of-the-art endoscopic diagnosis and treatment of early GI neoplasias.

Salzburg, Austria — Frieder Berr
Saku, Nagano, Japan — Tsuneo Oyama
Lyon, France — Thierry Ponchon
Shinjuku-ku, Tokyo, Japan — Naohisa Yahagi
August 20, 2018

Acknowledgments

The special thanks of the editors and authors go to all who have relentlessly contributed to the text and figures of the book, in particular Dr. Tobias Kiesslich of Salzburg and Dr. Akiko Takahashi of Nagano, as well as to the staff of Springer US, Clinical Medicine publishers, especially Mr. Andy Kwan and Mr. Richard Hruska, senior editor, Clinical Medicine.

Salzburg, August 15, 2018 The editors

Contents

Contributors

Frieder Berr Department of Internal Medicine I, Paracelsus Medical University, Salzburg, Austria

Pierre H. Deprez Department of Hepato-Gastroenterologie, Cliniques Universitaires Saint-Luc, Université Catholique de Louvain, Brussels, Belgium

Jürgen Hochberger Department of Gastroenterology, Vivantes Klinikum Berlin Friedrichshain, Berlin, Germany

Motohiko Kato Division of Research and Development for Minimally Invasive Treatment, Cancer Center, Keio University School of Medicine, Shinjuku-ku, Tokyo, Japan

Tobias Kiesslich Department of Internal Medicine I & Institute of Physiology and Pathophysiology, Paracelsus Medical University, Salzburg, Austria

Daisuke Kikuchi Department of Gastroenterology and Endoscopy Unit, Toranomon Hospital, Tokyo, Japan

Tadateru Maehata Division of Research and Development for Minimally Invasive Treatment, Cancer Center, Keio University School of Medicine, Shinjuku-ku, Tokyo, Japan

Atsushi Nakayama Division of Research and Development for Minimally Invasive Treatment, Cancer Center, Keio University School of Medicine, Shinjuku-ku, Tokyo, Japan

Daniel Neureiter Institute of Pathology, Paracelsus Medical University, Salzburg, Austria

Tsuneo Oyama Department of Endoscopy, Saku Central Hospital Advanced Care Center, Saku, Nagano, Japan

Thierry Ponchon Department of Digestive Diseases, Hôpital Eduard Herriot, Lyon, France

Hans Seifert Department of Internal Medicine – Gastroenterology, University Hospital Oldenburg, Oldenburg, Germany

Takashi Toyonaga Department of Endoscopy, Kobe University Hospital, Kobe, Japan

Toshio Uraoka Department of Gastroenterology and Hepatology, Gunma University Hospital, Maebashi, Prefecture Gunma, Japan

Andrej Wagner Department of Internal Medicine I, University Hospital, Paracelsus Medical University, Salzburg, Austria

Naohisa Yahagi Division of Research and Development for Minimally Invasive Treatment, Cancer Center, Keio University School of Medicine, Shinjuku-ku, Tokyo, Japan

Part I
General Principles of Endoscopy for Early Gastrointestinal Neoplasias

Chapter 1
Endoscopic Detection and Analysis of Mucosal Neoplastic Lesions: Enhanced Imaging and Tumor Morphology

Frieder Berr, Thierry Ponchon, and Toshio Uraoka

1.1 Introduction

Worldwide, the gastrointestinal (GI) tract is the organ system with the highest cancer incidence (20.5% of all new cases) and annual mortality (22% = 1.81 Mio). Early endoscopic detection and resection has led to improved survival rates for colorectal and gastric cancer, especially for gastric cancer in Japan, where more than 70% are now detected as early gastric cancer [1, 2].

The majority of esophageal and gastric cancers and about 50% of colorectal cancers (CRC) develop from flat precursor lesions [3, 4]. However, small (5–10 mm) or minute (<5 mm) flat neoplasias are easily missed on standard upper or lower GI endoscopy. The miss rate of such lesions had been estimated to be up to 19% [5]. Detection of small early neoplasias requires familiarity with the endoscopic spectrum of neoplastic lesions on conventional white-light imaging (WLI)

F. Berr
Department of Internal Medicine I, Paracelsus Medical University, Salzburg, Austria
e-mail: frieder.berr@pmu.ac.at

T. Ponchon
Department of Digestive Diseases, Hôpital Eduard Herriot, Lyon, France
e-mail: thierry.ponchon@chu-lyon.fr

T. Uraoka (✉)
Department of Gastroenterology and Hepatology, Gunma University Hospital, Maebashi, Prefecture Gunma, Japan
e-mail: turaoka@a3.keio.jp

F. Berr et al. (eds.), *Atlas of Early Neoplasias of the Gastrointestinal Tract*,
https://doi.org/10.1007/978-3-030-01114-7_1

[3, 6], as well as image analysis with the proper use of magnifying and image-enhanced endoscopy (IEE) [7], such as chromoendoscopy (CE) and narrow-band imaging (NBI) techniques [8–12]. Endoscopic microsurface (S) and microvascular (V) architecture have been characterized in normal mucosa and neoplasias by surface microscopic morphometry in comparison with magnified IEE images [13–15].

1.2 Standard Endoscopy and Chromoendoscopy Techniques

Image quality depends on *resolution* and *contrast*. Contrast is the ratio of brightness (light density) between a pattern and its background. Resolution is determined by the pixel number of the image sensor chip (CCD = charge-coupled device) and the optical lens system, as well as the pixel capacity of the video processor and the display monitor; therefore, resolution is enhanced by high-definition endoscopy (HD > 850 000 pixel), thus improving the detection rate of flat neoplasias. Contrast is increased by surface staining (chromoendoscopy, CE, e.g., with indigo carmine) or narrow-band spectral image (NBI) endoscopy [8, 11]. Most video endoscopy systems use a bright xenon lamp as a white light source. But two different systems for color reproduction are in use: the color CCD system with tiny red-green-blue (RGB) color filters in each CCD pixel, used in Western countries (simultaneous RGB system); and the RGB sequential imaging system using a monochromatic (black and white) CCD and color transformation of the light pulses in the video processor (Fig. 1.1a, b), used in Japan, East Asia, and the UK. The color CCD system shows better motion imaging, and the RGB sequential system yields better resolution [11].

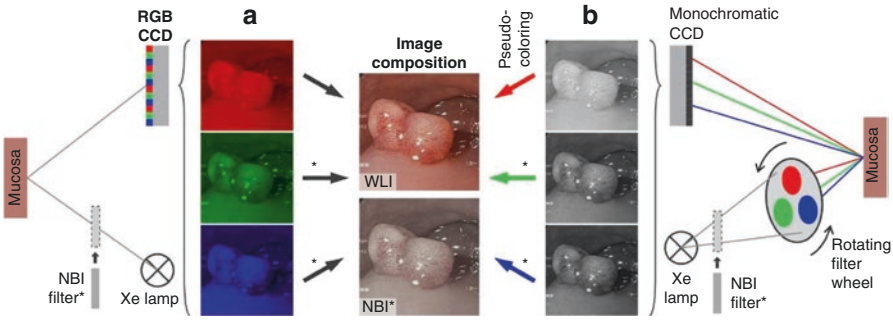

Fig. 1.1 (**a**) Schematic diagram of CCD-based simultaneous color imaging system (EVIS Excera III). *CCD* charge-coupled device. (**b**) Schematic diagram of red-green-blue (RGB) sequential imaging system (EVIS Lucera Spectrum)(Olympus Medical System Co., Tokyo, JP). Insertion of an NBI filter into the Xe-light path eliminates red light and illuminates mucosa with less intense, dual narrow-spectrum light of 415 nm and 540 nm – interacting with the two absorption maxima of hemoglobin. (Modified from Uedo et al. [11])

For *NBI observation* (Fig. 1.1a,b), a narrow band filter is switched into the light path. From the broadband white light of the xenon lamp, two bands with reduced light intensity are split, blue with wavelength of 415 nm and green with 540 nm, corresponding to the absorption peaks of hemoglobin. The light scattered in and reflected from the mucosa shows greenish blue color, and its absorption by hemoglobin in blood vessels shows the complimentary pseudocolor, i.e. brownish and dark cyan. The 415 nm blue light band highlights brownish-appearing capillaries in the lamina propria mucosae (LPM), and the more tissue-penetrating 540 nm green band shows cyan pseudocolored veins in the submucosa, together contrasting the superficial vascular (V) architecture [11, 15] (compare Fig. 1.4). On the other hand, Blue Light Imaging (BLI, Fujifilm Corp., Tokyo) generates similar light bands as NBI without a filter by using four LED (blue-violet, 415 nm / blue / green / red), and thus enhances magnifying surface (S) and vascular (V) imaging [8]. Based on the principles of NBI, alternative processing systems use computer-based filtering of reflected light for spectral light bands in the image processor, e.g., flexible spectral imaging color enhancement (FICE, Fujifilm Corp., Tokyo) or i-Scan tone enhancement (TE) mode (Pentax Medical Corp.,Tokyo) [10, 16].

1.3 Standard White Light Imaging (WLI) and Chromoendoscopy (CE)

Screening and surveillance use light-intense WLI endoscopy for *detection* of early neoplasias focusing on changes in *surface structure* (epithelial architecture) and/or *color* of the mucosa [17]. The more reddish color of neoplastic lesions is due to increased vascular density of the lamina propria mucosa (LPM), decreased glandular layer, or both alterations combined; a more pale color reflects increased gland density / neoplastic cell infitration, diminished vascularized connective tissue of the LPM, or both factors combined. Rarely, neoplasias display the same color as the mucosa. The *analysis* of suspicious lesions is facilitated by CE and HD endoscopy and often is feasible only with enhanced magnification imaging (60–120-fold) of microsurface (S) and microvascular (V) patterns in WLI and NBI or BLI technique [8, 18, 19].

Chromoendoscopy (CE) with acetic acid or indigo carmine enhances the surface structure, whereas Lugol (iodine) solution reacts with squamous epithelial cell membranes; methylene blue and crystal violet are internalized into columnar epithelial cells [3, 20]. Indications for and principles of CE are given in Table 1.1. For application of CE, wash the mucosa and lesion clean with water containing simethicone before absorptive stain – apply dye solution (e.g., 10 mL) for about 1 min, and wash again briefly before imaging. Esophageal squamous neoplasias show Lugol-*unstained* area on WLI, and appearance of slight pink coloring in unstained area after 1–2 min is highly specific for cancer (*pink coloring sign*) [21]. Neutralize the irritant action of Lugol solution immediately after iodine CE using sodium thiosulfate (5% aqueous sol., twice the volume of Lugol solution) [22]. Crystal violet staining is most accurate for irregular colonic microsurface (pit pattern type V; compare Chap. 11).

Table 1.1 Gastrointestinal chromoendoscopy and virtual chromoendoscopy (NBI or BLI)

A. Indications		
Location	**Neoplasia**	**Dye solution or VCE (NBI, BLI)**
Esophagus	Squamous cell cancer	Lugol[a] staining/NBI
	Barrett's HGIN, cancer	Acetic acid (AA)/indigo carmine (IC)/NBI
Stomach	Gastric adenoma, cancer	Indigo carmine (IC)/AIM[b]/NBI
Colon	Adenoma, HGIN, CRC	Indigo carmine (IC)/crystal violet/NBI
B. Application and principles of staining		
Principle	**Solution**	**Target structure/cells**
Reactive	Iodine-potassium iodide (0.75–1.0% aqu.) (Lugol solution)[a]	Squamous epithelial cell (SC) membranes; SC cancer: unstained area with clear demarcation line, "pink coloring sign" after 2 min
Contrasting	Indigo carmine (0.15% aqueous) AIM[b] (0.6% AA, 0.4% IC)	For macroscopic type and border of lesion AIM for identification of lesion border
Absorbed	Crystal violet (0.05% aqueous)[c]	Colonic epithelium

HGIN high-grade intraepithelial neoplasia, *VCE* virtual chromoendoscopy
[a]Avoid exposure of the larynx, iodine allergy, and hyperthyreosis! (comp. Chap. 7)
[b]AIM, freshly prepared mixture of 0.6% acetic acid and 0.4% indigo carmine [23]
[c]After spraying indigo carmine often combined (compare Chap. 11)

Note CE enhances surface pattern (S), NBI and BLI (or i-Scan TE mode) show microvascular architecture (V) and may indicate S structure of mucosal neoplasias, whereas CE better shows S structure and lateral margins of neoplasias.

1.4 Characteristics of Early Mucosal Neoplastic Lesions on WLI

Detection of a lesion depends on visible alterations in *surface structure* or *color* [6], whereas prediction of histopathological tumor (pT) category or invasiveness rests on *assessment* of three criteria – *macroscopic morphology*, *mucosal surface pattern* (S), and *microvascular pattern* (V) of the mucosa – and is performed with magnifying NBI or CE (see Sect. 1.5).

1.4.1 Macroscopic Classification (Paris-Japanese Classification)

The endoscopic classification developed in Japan [24] and promoted by international consensus in Paris is analogous for superficial neoplastic lesions of the esophagus, stomach, and colon [3, 20] (see Fig. 1.2a). Diagnostic failure mainly comes from mis-classification of type 0–IIa versus type 0–Is lesions, which is of minor importance for cancer miss rates, and from under-detection of type 0–IIc lesions, which is a major cause for missed cancer because even small 0–IIc neoplasias show a high rate of intramucosal cancer and progression to invasive cancer [3, 9].

Superficial protruding lesions (0–Ip, Isp, Is) are easily detectable. In the stomach, they comprise hyperplastic polyps (80–90%, multiple in chronic type B gastritis), adenoma (5–10%, with high risk of malignant foci), or differentiated adenocarcinoma (2–3%), inflammatory polyps (~2%, e.g. eosinophilic granuloma), rarely fundic gland polyps (e.g. in familial adenomatous polyposis), hamartomas (e.g. in juvenile polyposis or Peutz-Jeghers syndrome), or hereditary polyposes (e.g. Cowden syndrome, Cronkhite-Canada syndrome).

In the colon, most mucosal lesions are protruding; about two thirds are adenomas (some with high-grade intraepithelial neoplasia [HGIN] or early cancer), and one third are harmless hyperplastic polyps, which must not be confused with serrated adenoma. Submucosal tumors (lipoma, carcinoid [mainly in rectum], rare leiomyoma) are covered with normal or inflammatory mucosa; so are hamartomas (Peutz-Jeghers polyp and juvenile polyp) and inflammatory pseudopolyps.

Flat lesions, i.e. slightly elevated, completely flat, and slightly depressed lesions (IIa, IIb, IIc), are less striking on WLI and deserve continuous attention for changes in *color* and/or *surface structure* of the mucosa. In squamous and columnar epithelial esophagus and in the stomach, the majority of early cancers (75–80%) show flat

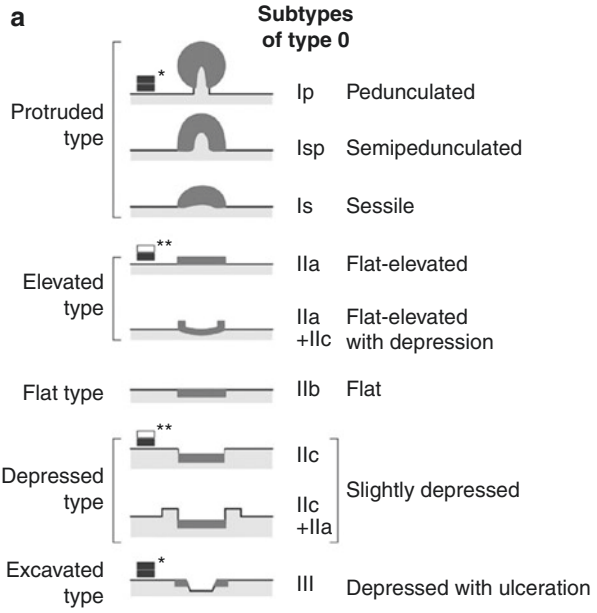

Fig. 1.2 (**a**) Endoscopic Paris classification of superficial neoplasias of the digestive tract (Modified acc. to [3, 20]): The macroscopic type is evident from the aspect of the lesion as compared with the size of a standard biopsy forceps (* closed cups of forceps = 2.5 mm; ** one jaw = 1.25 mm). Lesions are defined in relation to the adjacent surface as "protruding 0–I" (>2.5 mm↑ in columnar epithelium) and non-protruding, i.e., "flat-elevated = 0–IIa" (<2.5–0.5 mm↑), "flat = 0–IIb," and "depressed 0–IIc" (0.5–1.25 mm↓) or "excavated 0–III" (>1.25 mm↓). Composite lesions are described according to the combination of surface subtypes. In *esophageal* squamous epithelium, only *half* the sizes are used for the cutoff lines, e.g., ">1.25 mm↑ for 0–I," ">0.25 mm↑ for 0–IIa," ">0.25 mm↓ for 0–IIc," and ">0.5 mm↓ for 0–III." *, ** standard biopsy forceps (*gauge closed = 2.5 mm, **one jaw = 1.25 mm)

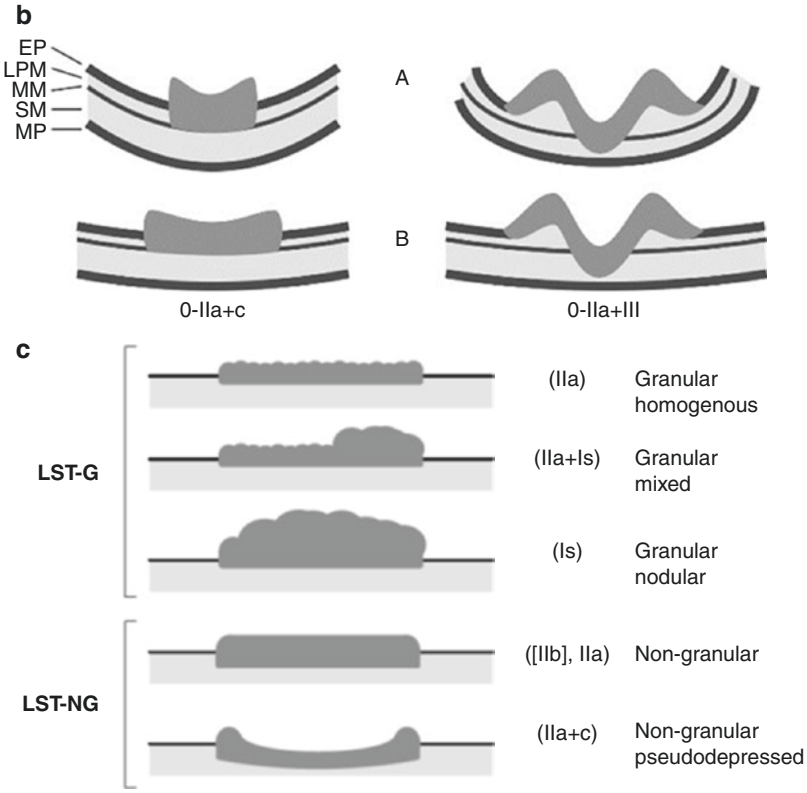

Fig. 1.2 (continued) (**b**) Desufflation (*A*)/insufflation (*B*) of a visceral organ provides information on depth of invasive growth. *Left*: Air-induced deformation of shape indicates infiltration of the muscularis mucosae (MM) layer. *Right*: Fixed shape of neoplasia indicates invasion of deep sm or MP layer. (**c**) Laterally spreading types of neoplasia (LSTs) [9]

lesions (IIa, IIb, IIc) [3]. Small early gastric cancers (EGC) typically display reddish type 0–IIc lesions when well differentiated, but small, pale type 0–IIb lesions, often with intact surface structure, when poorly differentiated. The latter are hard to detect and constitute about 15% of flat EGC in Japan and a higher fraction (up to 40%) in Western countries [25].

About 36% of *colonic neoplasias* present type 0–IIa flat lesions, and about 2% present type 0–IIc depressed lesions [9, 26]. As the tumor progresses in size and sm invasion, flat depressed neoplasia (0–IIc) may gain an elevated hyperplastic rim (types 0–IIc + 0–IIa) and become entirely elevated (types IIa + IIc) or ulcerated (0–III) in cases of deeply sm-invasive growth (Fig. 1.2a). Shape and deformation of a lesion during inflation/desufflation of the organ also provide information on invasive growth into the muscularis mucosae or deep sm/proper muscle layer (Fig. 1.2b).

Laterally spreading-type (LST) neoplasia (Fig. 1.2c) has been defined by Kudo et al. as a flat or elevated neoplastic lesion in the colorectum of more than 10 mm diameter [9]. These neoplasias (mostly adenomas) are barely distinguishable in color from the surrounding normal mucosa and can be quite flat or low elevated.

Chromoendoscopy with indigo carmine is advisable to demonstrate tumor extension. Uraoka et al. characterized the spectrum of LST, including nongranular-type LST with high probability of malignant foci (up to 50%) [27].

1.5 Magnifying and Image-Enhanced Endoscopy (IEE) for Analysis of Microarchitecture

1.5.1 Magnifying Endoscopy

Magnifying endoscopy with image enhancing endoscopy (IEE) techniques enables accurate diagnosis of early cancer lesions for appropriate curative resection technique [13, 28, 29]. High-definition (HD) endoscopes, even with the color CCD system, have a physical magnification up to 2 mm distance from the epithelial surface, yielding an optical magnification of 40-fold in dual-focus mode. With dual-focus endoscopes (e.g., GIF-H190Q or CF-H190Q for Exera III or GIF-HQ290 or CF-HQ290 for Lucera Spectrum, Olympus), the user can switch between standard mode and near mode (40-fold) for close focus observation with depth of field (DoF) of 2–6 mm. In combination with the 1.5-times digital zoom, these endoscopes offer 60-fold magnification. The Multi Light™ system (Eluxeo, Fujifilm) even allows switching from standard WLI or BLI to high-power magnifying (100×) WLI or BLI to obtain high-resolution IEE of micro-surface (S) and micro-vascular (V) structure. There are zoom endoscopes with adjustable image magnification up to 120-fold and depth of field (DoF) of 2–3 mm in both the sequential RGB and the simultaneous color CCD system. Moving the endoscope closer than 2 mm or further than 3 mm from the tissue causes the image to go out of focus. Therefore, a soft black hood as a distal attachment with depth equal to the DoFis essential on the zoom endoscope to keep the precise distance from the lens for clear, focused images (Fig. 1.3). To avoid contact bleeding,

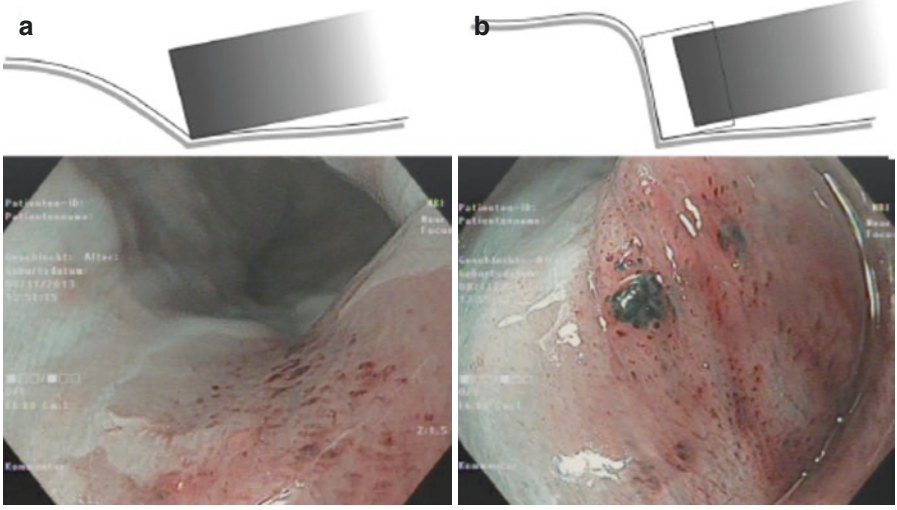

Fig. 1.3 M-NBI images of esophagus (**a**) without and (**b**) with distal attachment. (Modified from [11])

gently approximate the hood to the lesion and apply cautious suction/insufflation to optimize the focal distance. Observation under water with high magnification (60× – 120×) improves resolution and abolishes surface light reflection. In the stomach, there are two alternative techniques: (1) water filling of the stomach (e.g. with 500 mL water), or (2) water irrigation by injecting water from a syringe (20 or 50 mL) via a working channel into the distal hood when it is approximated to the target mucosa. The latter technique is also useful for acetic acid magnified CE of small lesions.

1.5.2 Image-Enhanced Endoscopy (IEE)

Narrow-band imaging (NBI), as well as *CE*, *augments the contrast* and enhances visibility of structures (IEE) while changing the image color [15, 30]. *NBI* based on hemoglobin absorbance images the microvessels in the superficial mucosal layer (lamina propria) and the submucosa [15, 29, 30] (Fig. 1.4), and sharpness of imaging depends on the index of hemoglobin color enhancement (IHb) [12]. The *structure enhancement function* improves image resolution on magnifying (M) observation in Olympus Lucera CV-260LS and Excera CV-190 *video processors*. There are two modalities (modes A and B) with eight levels each, and three of them can be preset. For the best structure enhancement settings see Table 1.2. The ELUXEO system (Fujifilm Corp., Tokyo) also has modes A and B with nine levels for BLI. The default setting for BLI is B4 for both standard and magnification.

The post-imaging digital filter technique (*i-Scan*, Pentax) needs tuning for enhancement of surface structure (SE mode) or of green-blue spectral bands for "tone enhancement" (TE) mode [16]. BLI, FICE, and *i-Scan* use principles established for NBI, and key findings reported for NBI also apply [8, 10, 16].

Key Points for Magnifying Endoscopy (60× – 130×):
- Proper structure enhancement settings of the video processor (Table 1.2)
- Soft distal hood (depth = DoF) to keep focal distance
- Water immersion (water filling or irrigation technique)
- Surface enhancement with acetic acid CE (Table 1.1, in irrigation technique).

Note Magnification (60-fold to 130-fold) combined with image-enhanced techniques (NBI, BLI, i-Scan, acetic acid, or crystal violet CE) yields maximum performance for diagnostic analysis of early neoplasias.

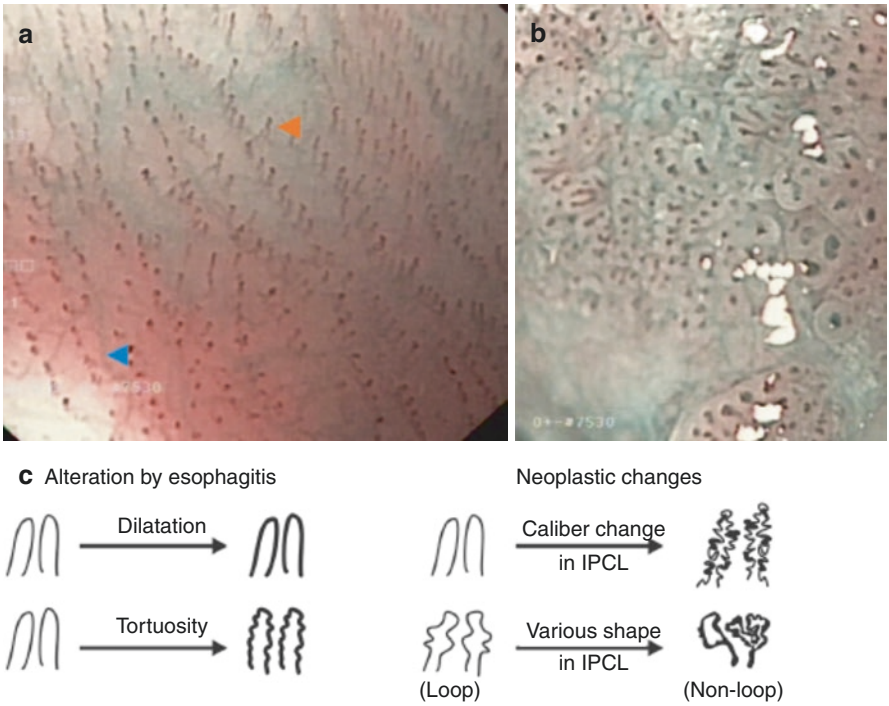

Fig. 1.4 Microvascular pattern (m-NBI, 60×) of squamous epithelial mucosa. (**a**) Normal esophagus. Faint submucosal collecting venules (cyan) ◀ and intrapapillary capillary loops (IPCL, light brown ◀) in LPM of squamous cell mucosa. (**b**) Neoplasia with HGIN. Disappearance of sm collecting venules, typical changes of IPCL (thickness, curling). (**c**) Basic alterations of schematic IPCL structure. (Modified from [11], permission granted by John Wiley & Sons Inc.)

Table 1.2 Structure enhancement settings (mode A vs. B, levels 1–8) [11, 12]

OLYMPUS	Excera III,CV-190	Lucera, CV-290
Standard WLI	A3 and A5	A5
M-WLI (>40-fold)	A8	A8 (or B8)
Standard NBI	B1 and B3	B1 and B3
M-NBI (>40-fold)	B8 (or A8)	B8

Color mode (level range 1–3): Level 1 for WLI, and for NBI level 1 and 3 in the GI tract

1.6 Capillary Structure of Squamous Mucosa and Neoplasias

Squamous epithelial esophagus displays rows of tiny reddish dots on WLI, which are identified on magnifying NBI as intrapapillary capillary loops (IPCL) in papillae of the mucosal LPM layer (Fig. 1.4a). Neoplasias in squamous epithelium

induce angiogenesis and change vascular architecture of IPCL visible on IEE as alterations of IPCL morphology (Fig. 1.4b). Basic abnormal changes are in diameter ("caliber change" by 2×; "thick vessel" by 3×), irregularity in shape (non-loop due to fusion/destruction of papillae). This sequence of angiogenic alterations by early neoplasias (Fig. 1.4b, c) is well visible in squamous epithelial esophagus (*see* Table 7.2) and, in analogous fashion, is known in early cancer of columnar cell–lined mucosa (see below).

Key Points for Intrapapillary Capillary Loops (IPCL)
- Caliber change (thickness)
- Tortuosity
- Loop shape (loop / non-loop)

Note Squamous epithelial esophagus is best screened with both WLI (on scope insertion) and NBI observation (on scope withdrawal), whereas oropharynx and hypopharynx are screened with NBI on scope insertion, and during expiration for better overview (compare Sect. 6.4.2).

1.7 Analysis by IEE of Columnar Epithelial Mucosa and Neoplasias

Columnar epithelial mucosa extends between the squamocolumnar junctions at cardia and anal channel and presents different surface patterns depending on the type of mucosal glands. Single-layered columnar epithelium (in large intestine with mucin-rich goblet cells) covers the surface of mucosa and glands. Mucosa contains tubular glands with pitlike orifices in the colorectum and gastric fundus/corpus (fundic-type mucosa), displaying on IEE a pattern of *regular pits* in an even mucosal surface. In the antrum and pylorus, and in cardia and Barrett's esophagus, the mucosal surface forms villi or ridges surrounded by groove-like crypts; therefore, the surface pattern is *villous* (tubular) or *gyrus* (ridgelike). In small bowel, the mucosal surface is entirely villous (tubular).

On *NBI* of *columnar epithelial mucosa* (Barrett's esophagus, stomach, and intestine), the surface pattern of marginal crypt epithelium is superimposed onto the capillary pattern of the lamina propria, yielding complex surface (S) and vessel (V) patterns (Fig. 1.5). *Colonic mucosa* exhibits a regular surface pattern of pits on magnifying NBI and indigo carmine CE (explained in Fig. 1.5), which differs from adenoma.

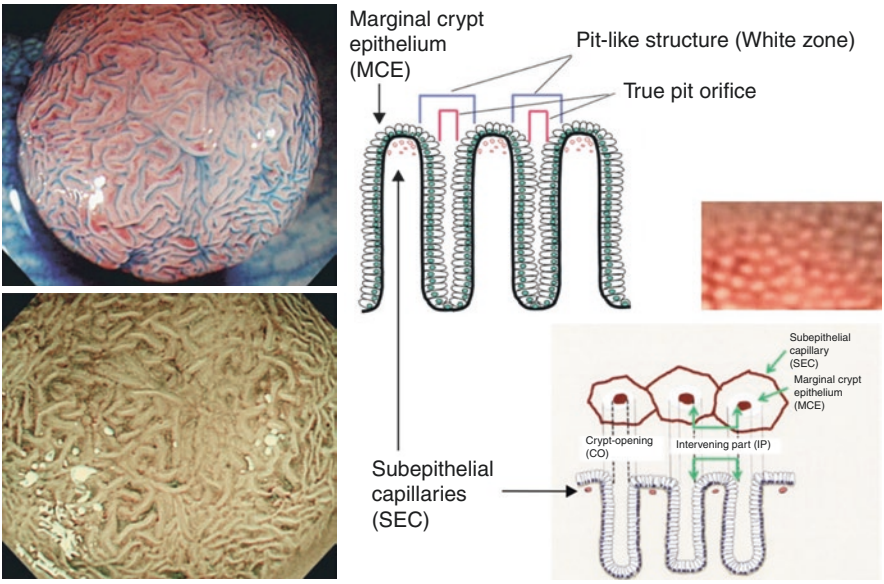

Fig. 1.5 Explanation of complex NBI patterns in columnar epithelial mucosa (*right side*; colon) and adenoma (*left side*). (Adapted from Tanaka et al. [32], permission granted by John Wiley & Sons Inc.). Magnifying colonoscopic images of normal mucosa (*right*) and tubulovillous adenoma (*left*, *top*: indigo carmine CE; *left*, *bottom*: NBI). The "white zone" (*WZ*) on the NBI image represents the perpendicularly illuminated layers of marginal crypt epithelium of glandular pits (the V pattern is extinct), which is the entire pitlike structure (*right panel*). An actual pit is hardly observed as a *dark dot* (mNBI 100×), because perpendicular illumination of the gland pit is rarely achieved. The vascular pattern (VP) of normal colonic mucosa is regular and brownish on NBI (*right upper panel*). Adenoma has a gyrous structure with ridges and groves (*left*)

1.7.1 Microarchitecture of Colonic Neoplasias

Adenomas in the gastrointestinal tract are defined on histology by cylinder epithelial cells with enhanced proliferation, *even* structure of pseudoglands, and *noninvasive* growth pattern (Fig. 1.6). These clonal epithelial neoplasms form different macroscopic types, e.g., flat types 0–IIb and 0–IIc or flat elevated types 0–IIa, which can also grow to sessile or polypoid adenoma or expansively spread out to larger, flat or flat-elevated, laterally spreading-type neoplasias (LST, in colon).

Note *Classic adenoma,* as compared with normal colonic mucosa on M-NBI (Fig. 1.6), is characterized by:

- *Regular surface pattern, SP* (evenly spaced WZ = MCE of pseudoglands)
- *Even but enhanced vascular pattern, VP* (reticular or spiral) around pseudoglands [15]
- *Clear margin* (without demarcation in surface relief)
- *Disappearance* of branched (dendritic) *sm vascular pattern*

Mucosal carcinoma arising in adenoma leads to irregular structures:

- *Irregular SP (uneven WZ, loss of structure* of crypt epithelium and pseudoglands)
- *Irregular VP* (sparse, curled vessel pattern due to destruction of pseudoglands)
- *Demarcation line* in surface *relief* (and *expansive nodule* or *encroachment*), if invasive into mucosal layer (Fig. 1.7a, c), or superficial submucosal (SM1) layer [19]

In general, the longer the adenomatous proliferation proceeds, i.e., with enlarging adenoma size, the greater the risk of malignant transformation. Even more so, the potential for cancerous transformation of colonic adenomas depends on histomorphologic type, increasing in the order of tubular, tubulovillous, villous, and serrated adenomas, and intraepithelial neoplasia (compare Fig. 2.2 and Table 2.1). Colorectal small depressed adenomas (types 0–IIc) tend to transform early to invasive adenocarcinoma that infiltrates the mucosa or sm layer. Some even arise as minute intraepithelial HGIN or carcinoma in situ [9].

These alterations of colonic mucosal surface and vessel structures induced by adenomatous and carcinomatous transformation have been characterized and classified as *pit pattern*s (*PP*) by Kudo [9] and *capillary pattern*s (*CP*) by Sano et al. [15] (Table 1.3; compare Fig. 11.2a–h). Combined analysis of vessel pattern

Table 1.3 Sano's capillary pattern types (CP) renamed as vessel types (V) in the Japan NBI Expert Team (JNET) classification using mNBI [19, 32]

Vessel type	V 1	V 2A	V 2B	V 3
CP type	CP I	CP II	CP IIIA	CP IIIB
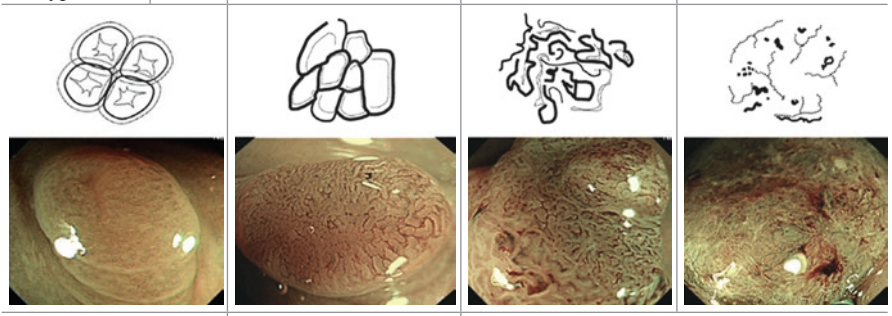				
Meshed capillary vessels, invisible (−) or normal		Meshed capillary vessels, regular (+)	Meshed capillary vessels, characterized by branching, curtailed irregularity & blind endings	
		Capillary vessels surround mucosal glands	Lack of uniformity High density of capillary vessels	Nearly avascular, or loose capillary vessels
Hyperplastic polyp[a]		Adenoma, LGIN	Ca-m[b], sm–superficial[c]	Ca sm – deep[d]

Permission granted by the Japan Gastroenterological Endoscopy Society/Digestive Endoscopy, and John Wiley & Co.

[a]normal hyperplastic polyp or sessile serrated polyp [19]

[b]HGIN, intramucosal cancer Ca-m

[c]sm superficial invasion (<1000 μm)

[d]sm deep invasion (≥1000 μm)

(V = CP) and surface pattern (S = PP) of colonic mucosal neoplasias allows prediction of malignancy and submucosal invasion with high accuracy (>90%). (See Chap. 11 for details.)

An international panel has simplified these two classifications to the *Narrow-Band Imaging International Colorectal Endoscopic (NICE) classification*, applicable for *standard endoscopy* (indigo carmine CE and NBI) without magnification [32, 33]. The NICE classification has been evaluated, but only tentatively differentiates superficial from deep sm-invasive (≥sm2) cancer [33]. Based on magnifying NBI, the Japan NBI Expert Team (JNET) reached consensus on the *JNET classification* to better discriminate superficial from deep sm-invasive carcinoma [19] (Table 1.4).

Table 1.4 Relationship between Narrow-Band Imaging International Colorectal Endoscopic (NICE) classification[a], Sano's classification, and Japan NBI Expert Team (JNET) classification

NICE	Type 1	Type 2	Type 3
Color	Same or lighter than background	Brownish relative to background (verify color arises from vessels)	Brown to dark brown relative to background; sometimes patchy whiter areas
Vessels	None, or isolated lacy vessels might be present coursing across the lesion	Thick, brown vessels surrounding white structures[b]	Area(s) with markedly distorted or missing vessels
Surface pattern	Dark or white spots of uniform size or homogenous absence of pattern	Oval, tubular or branched white structures surrounded by brown vessels	Areas with distortion or absence of pattern
Most likely pathology	Hyperplastic	Adenoma, HGIN, intramucosal cancer[c]	Deeply submucosa invasive cancer
Sano's CP classification[d] [29]	Type I	Type II / Type IIIA	Type IIIB
JNET classification[e]	Type 1	Type 2A / Type 2B	Type 3

Modified from Tanaka et al. [32], Sano et al. [19]

[a]Can be applied using colonoscopes both with and without optical magnification

[b]These structures might be the pits and the epithelium of the crypt opening

[c]Type 2 consists of the Vienna classification types 3, 4, and superficial 5. In some countries (e.g., the USA), type 2 includes all adenomas with either low-grade or high-grade dysplasia. High-grade dysplasia in the USA includes adenomas with carcinoma in situ or intramucosal carcinoma. In Japan, intramucosal cancer might be termed *cancer* rather than high-grade dysplasia. Some lesions with superficially submucosal invasive cancer might also have type 2 appearance

[d]For description of Sano's types compare Table 1.3

[e]Types 1–3 of JNET classification correspond to types I to IIIB of Sano's CP classification

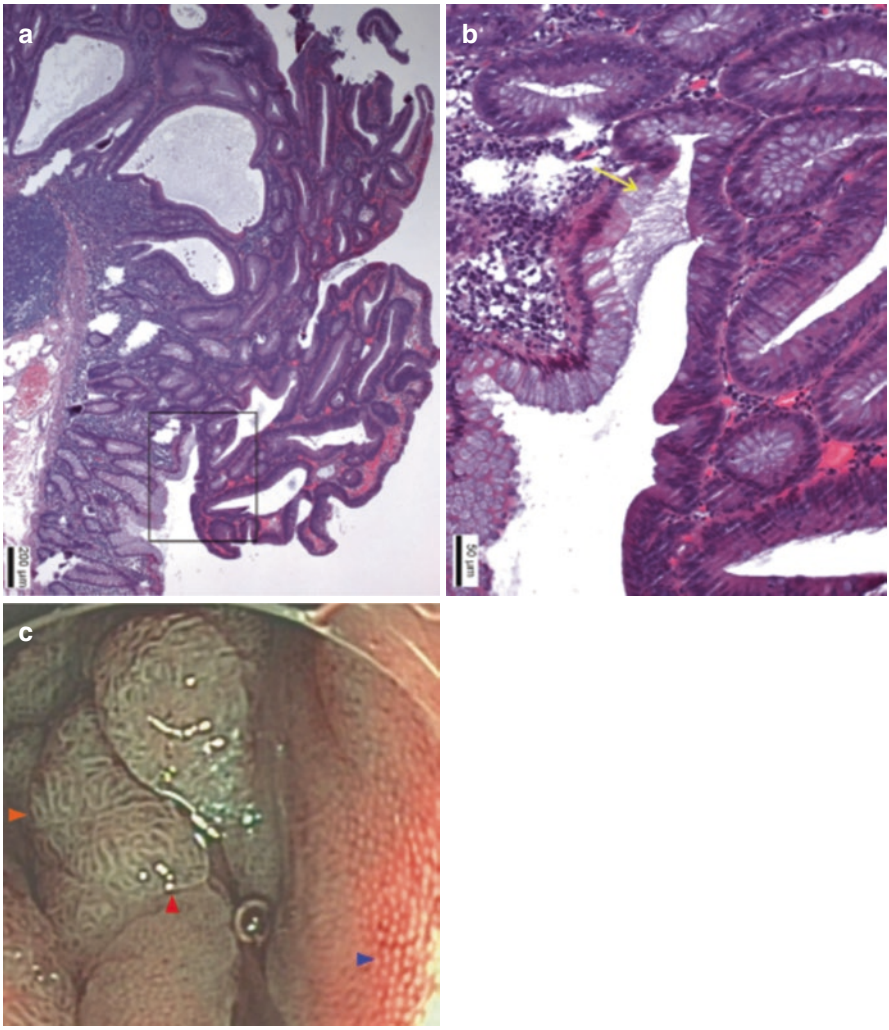

Fig. 1.6 (**a**) *Classic tubular adenoma* in the colon exhibits a noninvasive growth pattern of regular tubular glands. Coherent expansive growth of transformed epithelium creates pseudoglands with single-layered surface epithelium (*even WZ*) and may lead to protruding mucosal neoplasia 0–IIa or Isp (HE stain). (**b**) Magnified inset from **a**,: showing a sharp transition (*yellow arrow*) with even surface (*clear margin, even surface*) from colonic epithelium (*left side*) to adenomatous colonocytes (*right side*), which show an enhanced nucleus/cytoplasm ratio, loss of basal polar orientation, and clonal proliferation without goblet cells. (Courtesy Dr. Daniel Neureiter). (**c**) Magnifying NBI (60×) reveals normal colonic mucosa (*right side*, ▶) with round white dots representing marginal crypt epithelium (WZ) of tubular glands and a fine, brownish network of capillaries around glands in the mucosal layer. Top and left sides (▶) show protruding adenoma (0–Is) with a large tubular surface structure displaying even bands of WZ and ridgelike bands of brownish VP in LPM of adenomatous pseudogland tubule. The adenoma has a clear sharp margin (▲) to columnar mucosa

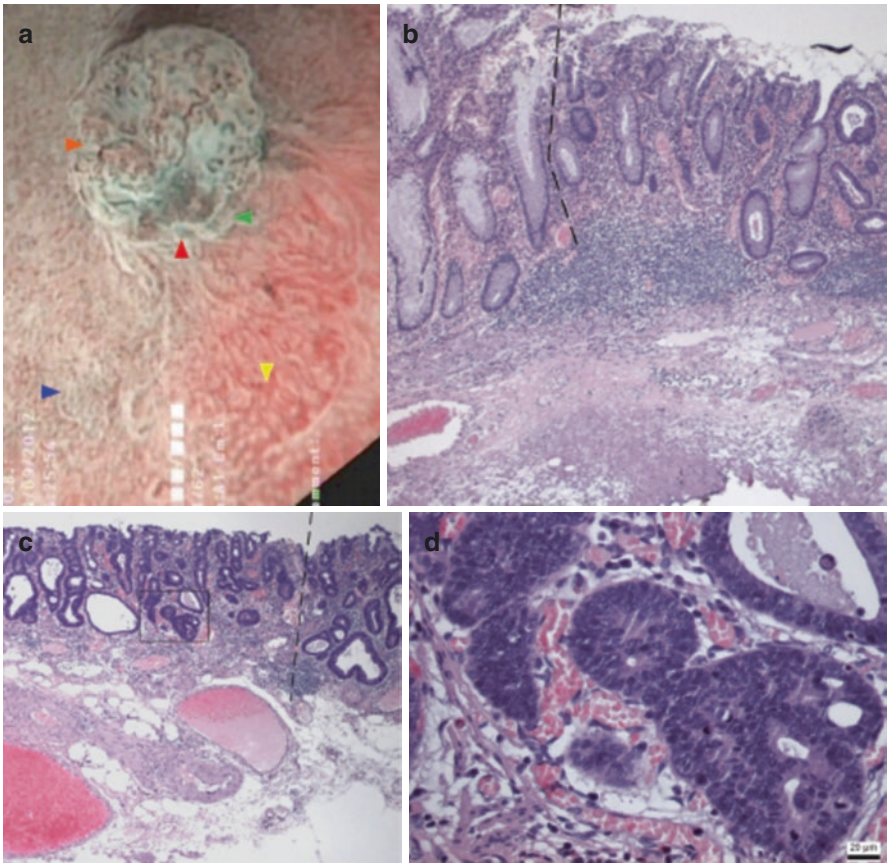

Fig. 1.7 (**a**) Colonic LST 0–IIb presenting ▶ meshed capillary pattern (CP II) and small nodule 0–IIa (▲ with demarcation line) displaying ▶ irregular dense CP (IIIA) and ◀ irregular sparse CP IIIB with thick vessels (magnifying NBI, 80×). ESD showed tubular adenoma with low-grade intraepithelial neoplasia (LGIN) in 0–IIb and adenocarcinoma pTis (LPM) in nodule IIa. *Vertical arrows* mark margins between hyperplastic and neoplastic mucosa (▼ in (**a**) represents *dotted line* in (**b**)) and between adenoma and intramucosal adenocarcinoma [G2, T1a LPM] (▲ in (**a**) marks *dotted line* in (**c**)). (**b**) Transition (*dotted line*) from hyperplastic mucosa with goblet cell–rich pits (*left*) to tubular adenoma with regular pseudoglands, lack of goblet cells, augmented capillaries in mucosa, LPM. (**c**) Transition (*dotted line*) from adenoma (*right*) to adenocarcinoma (*left*; *insert* = *d*) with irregular glands and thick microvessels. (**d**) Adenocarcinoma [G2, T1a LPM] (insert in **c**, 10× more magnified). (Courtesy Dr. Daniel Neureiter)

1.7.2 Microarchitecture of Gastric Mucosa and Neoplasia

Gastric mucosa exhibits columnar cell–lined epithelium with mucosal areas (*areae gastricae*) separated by fine grooves. The mucosa of the gastric fundus and corpus is lined with fundic-type glands presenting a regular pattern of round or oval pitlike

gland openings surrounded by a brownish reticular network of microcapillaries on M-NBI (Fig. 1.8a, normal margin; Fig. 1.9). By contrast, the distal corpus and antropyloric region bear pyloric-type glands showing a villous surface and a regular open-loop pattern on M-NBI (Fig. 1.10a, normal margin). Normal *fundic*-type mucosa without gastritis displays a regular red pattern of starfish-like submucosal collecting venules (regular arrangement of collecting venules, *RAC*) on WLI, which vanishes in severe gastritis. Severe chronic *atrophic gastritis* – at increased risk for cancer – presents a prominent *submucosal* vascular pattern on WLI, and often intestinal metaplasia presenting mainly as whitish areas with uncertain margin and loss of sm vascular pattern on WLI, with light blue crests (*LBC* = brush border in cells) in the white zone of marginal epithelium on magnifying NBI [31]. (Compare Chap. 9.)

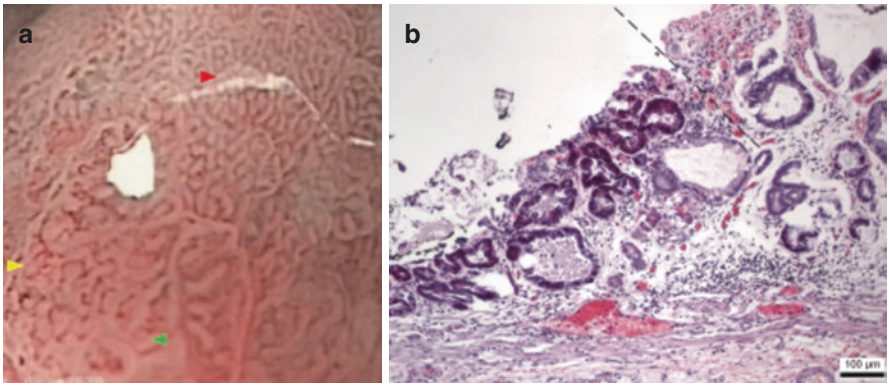

Fig. 1.8 Well-differentiated adenocarcinoma (WDAC, tub, G1, pT1a MM) 0–IIa, gastric corpus. (**a**) NBI (100-fold): ▶ fundic mucosa (top right side: oval pit pattern); ▶ clear margin (*demarcation line*) due to expansion of WDAC/MDAC as coherent tumor cell cluster; ◀ fine network with irregular microvascular pattern (VP). For respective VP, compare Fig. 1.9. (**b**) HE stain shows sharp margins (*dotted line*) to WDAC (*left side*). (Courtesy Dr. Daniel Neureiter)

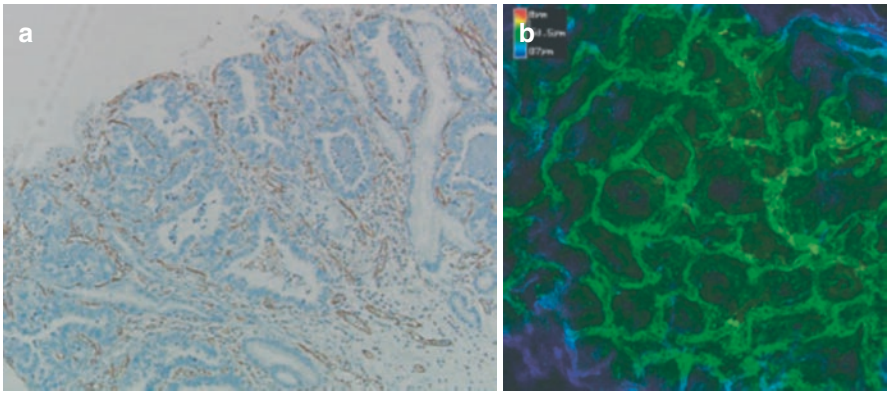

Fig. 1.9 (**a**) Histology of gastric WDAC demonstrates *coherent expansion* of mucosal cancer with relatively regular pseudogland and capillary structure (VP). (**b**) In analogy, intact VP of gastric WDAC, as revealed by laser scanning microscopy (LSM) of HE stain after CD31-immunohistological staining of capillary endothelia, displays a nearly regular network VP. (Permission of Thieme/Endoscopy [14])

Small early gastric cancer (<10 mm) (EGC) is easily missed when WLI does not focus on *discolored spots*, the hallmark for flat EGC, because only 15–20% are elevated lesions (0–IIa/Is, usually differentiated adenocarcinoma [AC]), but 80–85% are tiny flat (0-IIb) or depressed (0-IIc) lesions (Figs. 1.8 and 1.10). Up to 40% of small flat EGC is poorly differentiated diffuse-type AC (grading G3, PDAC) [25]. Unfortunately, most small PDAC is difficult to detect on WLI or even M-NBI, owing to pale or isochrome aspect. The histology explains why: The vascular pattern in the LPM often is sparse, and cancer cells diffusely spread in LPM and sm, hiding the vascular pattern (Figs. 1.10 and 1.11), and epithelium and gland openings may be preserved as normal on the luminal surface.

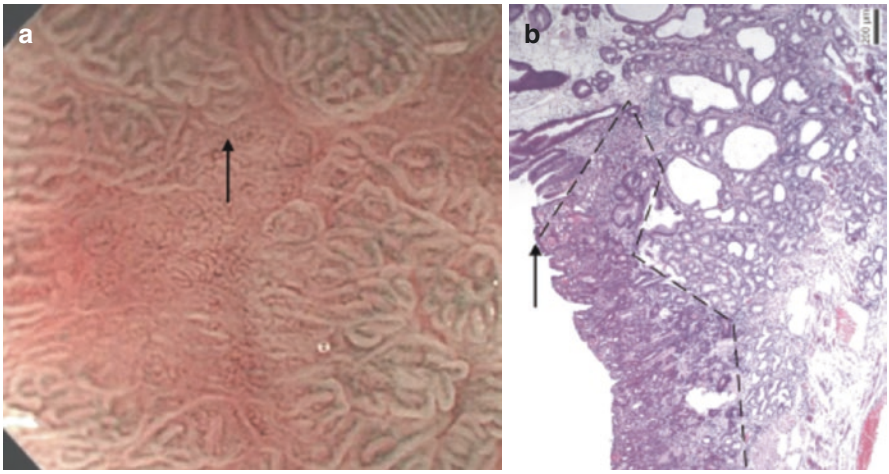

Fig. 1.10 (**a**) Poorly differentiated, diffuse-type early gastric cancer (PDAC). Absent microsurface structure, sparse VP with corkscrew-like irregular microvessels, with encroachment (*arrow*) (M-NBI), surrounded by pyloric-type mucosa with villous SP. (Permission of John Wiley and Sons/J Gastroenterol Hepatol [34]). (**b**) Histology of another PDAC (*left side of dotted line*) with surface encroachment (*arrow*) and undermining of mucosal margin, loss of surface gland structure, and LPM layer diffusely infiltrated by cancer cells. (Courtesy Dr. Daniel Neureiter)

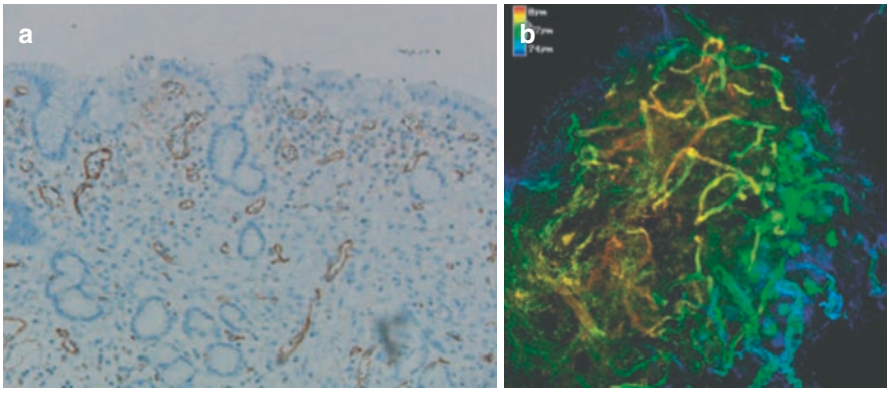

Fig. 1.11 Microarchitecture of small, depressed-type EGC of diffuse type with poorly differentiated grading (PDAC). (Permission of Thieme/Endoscopy [14]). (**a**) Histology of PDAC, HE stain, and CD31 immunostain of endothelium. (**b**) Laser surface microscopic reconstruction of VP in LPM layer of similar undifferentiated AC (PDAC) with a sparse, irregular capillary pattern and some corkscrew vessels

The vascular pattern (VP) shows a scanty and regular periglandular capillary network (mesh) in normal corpus/fundus mucosa with tubular glands, and spiral capillary patterns in normal antrum/pylorus mucosa covered with surface villi or ridges (Figs. 1.8 and 1.10). Early differentiated adenocarcinoma usually displays prominent irregular mesh VP and irregular surface pattern (SP) on magnifying NBI (Fig. 1.8). By contrast, in small 0–IIc lesions, a non-reticular, often sparse VP signals intramucosal poorly differentiated adenocarcinoma (PDAC, Fig. 1.10) or deep sm invasion of early well-differentiated AC (specificity 85%).

Correct mapping of *tumor extension* of EGC is necessary for endoscopic resection with free margins. Magnifying NBI helps to distinguish tumor margins from surrounding normal mucosa in cardia-type EGC, or more frequently from atrophic mucosa with intestinal metaplasia in chronic *Helicobacter pylori*–induced or autoimmune gastritis [18]. Surface enhancement using CE with acetic acid–indigo carmine mixture is very helpful for mapping of differentiated-type adenocarcinoma but tends to obscure pale-type 0–IIb small PDAC. (Compare Chap. 9)

Magnifying WLI followed by magnifying NBI endoscopy achieves >90% specificity and accuracy for endoscopic diagnosis of type 0–IIc small mucosal gastric adenocarcinoma and improves differential diagnosis for small flat or depressed lesions caused by chronic atrophic gastritis [18, 35]. The analysis of SP and VP in EGC is detailed in Chap. 9.

Note In stomach, assessment of SP and VP with M-NBI differentiates with high accuracy (>90%) [18, 35–37]:

- Non-neoplastic *versus* neoplastic mucosa
- Adenoma or differentiated mucosal adenocarcinoma (HGIN, T1 m/sm1) *versus* deeply sm-invasive carcinoma (≥sm2)

1.7.3 Microarchitecture of Columnar Mucosa-Lined Esophagus

Barrett's esophagus (BE) is an area of columnar epithelium-lined esophagus (*CLE*) extending for more than 1 cm oral to the gastroesophageal junction, which corresponds to the oral end of the gastric folds (Western definition) or the distal end of the longitudinal palisade vessel pattern (IPCL) in the esophagus (Japanese definition). According to the US definition, CLE with goblet cells on biopsy proves specialized intestinal metaplasia (SIM) which is required for diagnosis of BE in CLE. According to the Japan and British Gastroenterological Societies, BE is defined by CLE (without or with goblet cells). CLE increases the risk for adenocarcinoma of the esophagus or gastroesophageal junction to a similar extent in the absence or the presence of goblet cells [38–40]. In fact, even islets of columnar epithelial mucosa in an irregular Z-line (so-called *ultrashort BE*) may carry an increased risk of cancer, like non-goblet CLE [40] (Fig. 1.12).

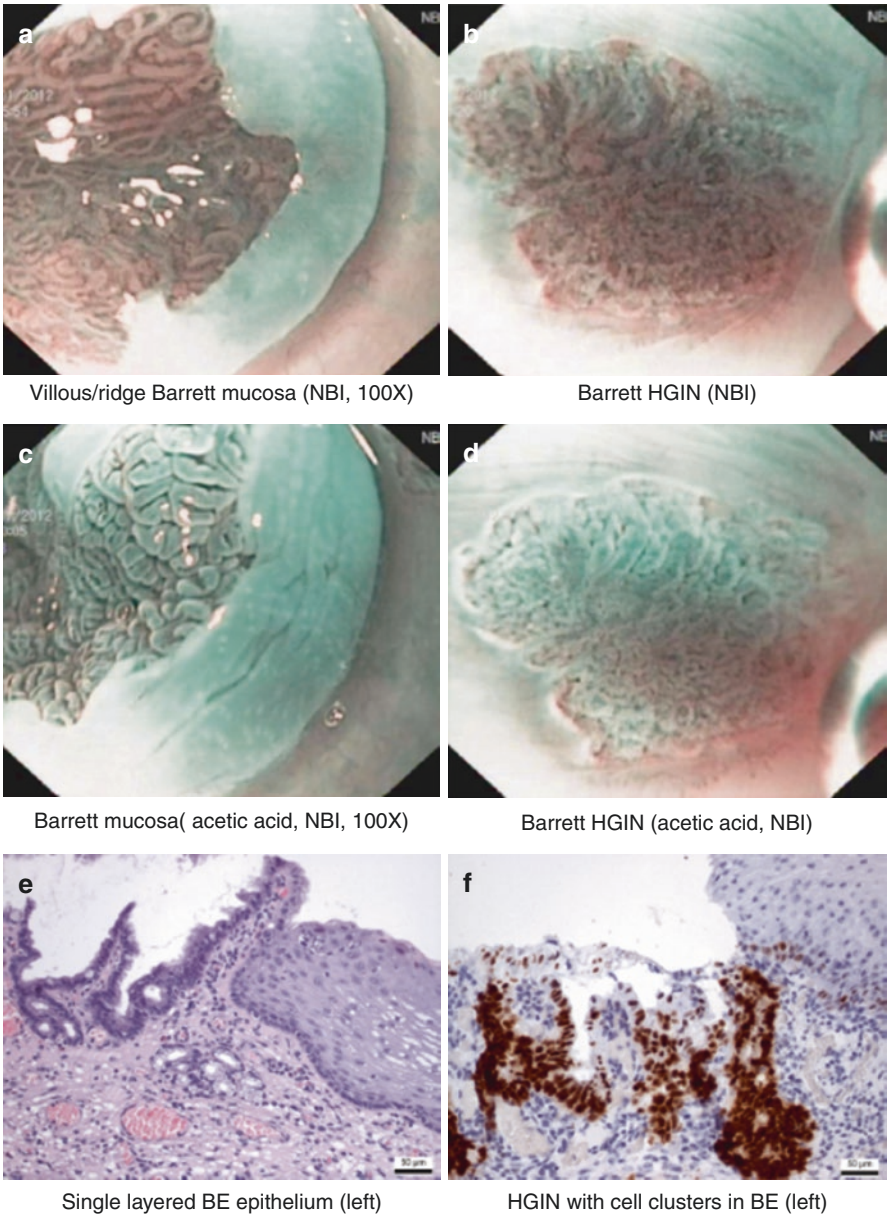

Fig. 1.12 Typical case of Barrett's mucosa with HGIN (Courtesy of Dr. H.P. Allgaier). *Left panels* (**a**, **c**, **e**): Linear WZ in villous/ridge-type Barrett's mucosa with (**a**) regular helix-like CP on M-NBI (100×); (**c**) even SP after 1.5% acetic acid; (**e**) margin of single-layered BE epithelium on the left side (HE stain, 100×). *Right panels* (**b**, **d**, **f**): HGIN in BE with irregular (**b**) CP, (**d**) SP, and (**f**) clusters of dysplastic cylinder cells. (**e**, **f**) HE stain after ESD, (**f**) with p53 immunohistochemistry. (Courtesy of Dr. Tsuneo Oyama, Nagano; and Dr. Daniel Neureiter, Salzburg)

Reports from Japan on the microsurface pattern (SP) and vascular pattern (VP) of Barrett's neoplasia are scarce because of its very low prevalence there, and the characterization of neoplastic alterations of surface structure lags behind that in colonic and gastric mucosa. At least four classifications of SP and VP of CLE mucosa are known [41–45], but none is universally accepted. In general, CLE shows five different regular patterns (round pits and tubular, linear, villous, or atrophic-absent surface patterns) (*See* Table 8.2). Linear/villous mucosal surface with "light blue crests" (LBC) on magnifying NBI is highly (~90%) sensitive and specific for specialized intestinal metaplasia (SIM) [31].

Early malignant neoplasias are mostly flat lesions (0–IIa–c, 85%) and hard to detect as minute (≤5 mm) or small lesions in Barrett's mucosa [46]. Basically, any slight alteration in reddish color or uneven surface relief on WLI must be analyzed with magnifying NBI endoscopy (>60×) and surface enhancement with acetic acid (*see* Fig. 1.12). *Neoplastic areas* (HGIN, early cancer), type 0–IIa–c, exhibit uneven surface relief and an irregular, speckled white zone of marginal epithelium, combined with irregularities in VP (irregular loop or spiral pattern) and clear margin of the suspicious area within surrounding BE mucosa [41, 43] The diagnosis of neoplasia should still be confirmed by targeted biopsy.

Note Irregular SP and VP in CLE distinguish with accuracy of 80–85% [41, 43, 45] between:

- Nonneoplastic CLE (−/+SIM) *versus* differentiated mucosal neoplasia (HGIN, T1 m, or sm1 adenocarcinoma)
- Deep submucosal invasion (≥sm2) of early cancer with severely irregular SP (destruction of gland structure) and CP (sparse and thick vessels)

Acknowledgments The contribution of cases or images by Dr. Hans-Peter Allgaier, Freiburg, Germany; Dr. Gerhard Kleber, Aalen, Germany; Dr. Tsuneo Oyama, Saku Central Hospital, Nagano, Japan; and Dr. Daniel Neureiter, University Institute of Pathology, Salzburg, Austria, is gratefully acknowledged.

References

1. Ferlay J, et al. Cancer incidence and mortality worldwide: sources, methods and major patterns in GLOBOCAN 2012. Int J Cancer. 2015;136:E359–86.
2. Inoue M, et al. Epidemiology of gastric cancer in Japan. Postgrad Med J. 2005;81:419–24.
3. The Paris endoscopic classification of superficial neoplastic lesions: esophagus, stomach, and colon: November 30 to December 1, 2002. Gastrointest Endosc. 2003;58:S3–43.
4. George SM, et al. Classification of advanced colorectal carcinomas by tumor edge morphology: evidence for different pathogenesis and significance of polypoid and nonpolypoid tumors. Cancer. 2000;89:1901–9.
5. Heresbach D, et al. Miss rate for colorectal neoplastic polyps: a prospective multicenter study of back-to-back video colonoscopies. Endoscopy. 2008;40:284–90.
6. Yao K, et al. Development of an e-learning system for teaching endoscopists how to diagnose early gastric cancer: basic principles for improving early detection. Gastric Cancer. 2017;20(Suppl 1):S28–38.

7. Kaltenbach T, et al. American Gastroenterological Association (AGA) Institute technology assessment on image-enhanced endoscopy. Gastroenterology. 2008;134:327–40.
8. Dohi O, et al. Diagnostic ability of magnifying endoscopy with blue laser imaging for early gastric cancer: a prospective study. Gastric Cancer. 2017;20:297–303.
9. Kudo S, et al. Colonoscopic diagnosis and management of nonpolypoid early colorectal cancer. World J Surg. 2000;24:1081–90.
10. Osawa H, et al. Present and future status of flexible spectral imaging color enhancement and blue laser imaging technology. Dig Endosc. 2014;26(Suppl 1):105–15.
11. Uedo N, et al. Role of narrow band imaging for diagnosis of early-stage esophagogastric cancer: current consensus of experienced endoscopists in Asia-Pacific region. Dig Endosc. 2011;23(Suppl 1):58–71.
12. Uraoka T, et al. Narrow-band imaging for improving colorectal adenoma detection: appropriate system function settings are required. Gut. 2009;58:604–5.
13. Kudo S, et al. Pit pattern in colorectal neoplasia: endoscopic magnifying view. Endoscopy. 2001;33:367–73.
14. Nakayoshi T, et al. Magnifying endoscopy combined with narrow band imaging system for early gastric cancer: correlation of vascular pattern with histopathology (including video). Endoscopy. 2004;36:1080–4.
15. Sano Y, et al. Magnifying observation of microvascular architecture of colorectal lesions using a narrow-band imaging system. Dig Endosc. 2006;18:s44–51.
16. Kodashima S, et al. Novel image-enhanced endoscopy with i-scan technology. World J Gastroenterol. 2010;16:1043–9.
17. Yao K, et al. Development of an e-learning system for teaching endoscopists how to diagnose early gastric cancer: basic principles for improving early detection. Gastric Cancer. 2017;20:28–38.
18. Muto M, et al. Magnifying endoscopy simple diagnostic algorithm for early gastric cancer (MESDA-G). Dig Endosc. 2016;28:379–93.
19. Sano Y, et al. Narrow-band imaging (NBI) magnifying endoscopic classification of colorectal tumors proposed by the Japan NBI Expert Team. Dig Endosc. 2016;28:526–33.
20. Update on the Paris classification of superficial neoplastic lesions in the digestive tract. Endoscopy. 2005;37:570–8.
21. Ishihara R, et al. Quantitative analysis of the color change after iodine staining for diagnosing esophageal high-grade intraepithelial neoplasia and invasive cancer. Gastrointest Endosc. 2009;69:213–8.
22. Kondo H, et al. Sodium thiosulfate solution spray for relief of irritation caused by Lugol's stain in chromoendoscopy. Gastrointest Endosc. 2001;53:199–202.
23. Kawahara Y, et al. Novel chromoendoscopic method using an acetic acid-indigocarmine mixture for diagnostic accuracy in delineating the margin of early gastric cancers. Dig Endosc. 2009;21:14–9.
24. Japanese Research Society for Gastric Cancer. Japanese classification of gastric carcinoma First English ed. Tokyo: Kanehara & Co., Ltd; 1995.
25. Everett SM, et al. Early gastric cancer in Europe. Gut. 1997;41:142–50.
26. Rembacken BJ, et al. Flat and depressed colonic neoplasms: a prospective study of 1000 colonoscopies in the UK. Lancet. 2000;355:1211–4.
27. Uraoka T, et al. Endoscopic indications for endoscopic mucosal resection of laterally spreading tumours in the colorectum. Gut. 2006;55:1592–7.
28. Yao K, et al. Novel magnified endoscopic findings of microvascular architecture in intramucosal gastric cancer. Gastrointest Endosc. 2002;56:279–84.
29. Yoshida T, et al. Narrow-band imaging system with magnifying endoscopy for superficial esophageal lesions. Gastrointest Endosc. 2004;59:288–95.
30. Gono K, et al. Appearance of enhanced tissue features in narrow-band endoscopic imaging. J Biomed Opt. 2004;9:568–77.
31. Toyoda H, et al. Detection of intestinal metaplasia in distal esophagus and esophagogastric junction by enhanced-magnification endoscopy. Gastrointest Endosc. 2004;59:15–21.

32. Tanaka S, et al. Aim to unify the narrow band imaging (NBI) magnifying classification for colorectal tumors: current status in Japan from a summary of the consensus symposium in the 79th Annual Meeting of the Japan Gastroenterological Endoscopy Society. Dig Endosc. 2011;23(Suppl 1):131–9.
33. Hayashi N, et al. Endoscopic prediction of deep submucosal invasive carcinoma: validation of the narrow-band imaging international colorectal endoscopic (NICE) classification. Gastrointest Endosc. 2013;78:625–32.
34. Okada K, et al. Diagnosis of undifferentiated type early gastric cancers by magnification endoscopy with narrow-band imaging. J Gastroenterol Hepatol. 2011;26:1262–9.
35. Ezoe Y, et al. Magnifying narrowband imaging is more accurate than conventional white-light imaging in diagnosis of gastric mucosal cancer. Gastroenterology. 2011;141:2017–25. e2013.
36. Abe S, et al. Depth-predicting score for differentiated early gastric cancer. Gastric Cancer. 2011;14:35–40.
37. Tanaka K, et al. Features of early gastric cancer and gastric adenoma by enhanced-magnification endoscopy. J Gastroenterol. 2006;41:332–8.
38. Gatenby PA, et al. Relevance of the detection of intestinal metaplasia in non-dysplastic columnar-lined oesophagus. Scand J Gastroenterol. 2008;43:524–30.
39. Kelty CJ, et al. Barrett's oesophagus: intestinal metaplasia is not essential for cancer risk. Scand J Gastroenterol. 2007;42:1271–4.
40. Riddell RH, et al. Definition of Barrett's esophagus: time for a rethink--is intestinal metaplasia dead? Am J Gastroenterol. 2009;104:2588–94.
41. Anagnostopoulos GK, et al. Novel endoscopic observation in Barrett's oesophagus using high resolution magnification endoscopy and narrow band imaging. Aliment Pharmacol Ther. 2007;26:501–7.
42. Goda K, et al. Usefulness of magnifying endoscopy with narrow band imaging for the detection of specialized intestinal metaplasia in columnar-lined esophagus and Barrett's adenocarcinoma. Gastrointest Endosc. 2007;65:36–46.
43. Kara MA, et al. Detection and classification of the mucosal and vascular patterns (mucosal morphology) in Barrett's esophagus by using narrow band imaging. Gastrointest Endosc. 2006;64:155–66.
44. Sharma P, et al. The utility of a novel narrow band imaging endoscopy system in patients with Barrett's esophagus. Gastrointest Endosc. 2006;64:167–75.
45. Sharma P, et al. Development and validation of a classification system to identify high-grade dysplasia and esophageal adenocarcinoma in Barrett's esophagus using narrow-band imaging. Gastroenterology. 2016;150:591–8.
46. Pech O, et al. Prospective evaluation of the macroscopic types and location of early Barrett's neoplasia in 380 lesions. Endoscopy. 2007;39:588–93.